

Ultra-High Efficiency Co-Flow Jet Airfoil and the Transformative Aircraft

Dr. Ge-Cheng Zha*
Coflow Jet, LLC
PO Box 248661
Coral Gables, Florida 33124
E-mail: gzha@miami.edu
coflowjet.com
Tel: 305-284-3328

Summary

Coflow Jet(CFJ) airfoil is a zero-net mass-flux active flow control airfoil actuated by fluidic micro-compressors embedded inside the airfoil. A small amount of mass flow is withdrawn into the airfoil near the trailing edge, pressurized and energized by the micro-compressor actuators, and then injected near the leading edge in the direction tangent to the main flow. It is a self-contained high lift system with no moving parts(e.g. no flaps). It can achieve Super-Lift coefficient(e.g. 12) that far exceeds the theoretical limit defined by $C_{Lmax} = 2\pi(1 + t/c)$. It is virtually stall free with attached flow at angle of attack(AoA) as high as 70° . Furthermore, all these extraordinary benefits come with extremely low energy expenditure, which renders CFJ airfoil the unique flow control method that can not only enhance low speed takeoff/landing performance, but also radically increase aerodynamic productivity efficiency at cruise condition when the AoA is low and the flow is benign. In addition, the benefits are maintained to transonic regime for super-critical airfoil when shock waves appear. The CFJ airfoil is a promising technology to transform the future aviation. The ongoing DARPA project is to further mature this revolutionary technology.

1 Background

Green aviation with aircraft powered by electric batteries requires ultra-high aircraft aerodynamic efficiency to compensate the low energy density of batteries. Airfoil is the most fundamental aerodynamic element of aircraft. An aircraft wing is formed by a series of airfoils stacked along the span. With the success of NACA airfoils in the 1940's and the invention of the supercritical airfoil in the 1960's, manipulation of airfoil geometry to improve performance was thought to have reached limit. Attention in aircraft community is hence shifted to active flow control, which is hoped to enhance airfoil performance.

Overall, almost all the present airfoil active flow control methods are aimed at either suppressing flow separation(e.g. synthetic jets, dielectric-barrier discharge plasma actuators) or using Coanda effect (e.g. circulation airfoil) to increase the maximum lift coefficient. Few active flow control techniques are able to improve airfoil performance at cruise condition when the flow is benign at low AoA. Cruise is obviously the most important phase of a flight to reduce fuel consumption and emission pollution. Unfortunately, the airfoils used to cruise have remained virtually unchanged in the past five to seven decades for subsonic NACA airfoil and transonic supercritical airfoil.

The most recent concept of co-flow jet (CFJ) flow control airfoil, developed by Zha et al[1, 2, 3, 4, 5, 6, 7, 8, 9, 10, 11, 12, 13], appears to have changed this stagnancy of airfoil development of the past several decades. The CFJ airfoil achieves a radical lift augmentation, drag reduction and stall

* President, Professor, AIAA Associate Fellow, NASA NIAC Fellow, ASME Fellow

margin increase at low energy expenditure. It can not only achieve short takeoff and landing(STOL) performance with ultra-high maximum lift coefficient, but also significantly enhance cruise efficiency and cruise lift coefficient(wing loading) from subsonic to transonic conditions[10, 11, 12, 13]. Cruise wing loading that is much higher than conventional designs allows the CFJ aircraft to carry more fuel or batteries and thereby have a significantly longer range[10, 11]. The CFJ airfoil has great potential to revolutionize the conventional aircraft design from subsonic speed to transonic speeds.

2 Innovation: the Co-Flow Jet Airfoil

The CFJ airfoil has an injection slot near the leading edge(LE) and a suction slot near the trailing edge(TE) on the airfoil suction surface as sketched in Fig. 1. A small amount of mass flow is withdrawn into the airfoil near the TE, pressurized and energized by a pumping system inside the airfoil, and then injected near the LE in the direction tangent to the main flow. The whole process does not add any mass flow to the system and hence is a zero-net mass-flux flow control. It is a self-contained high lift system with no moving parts.

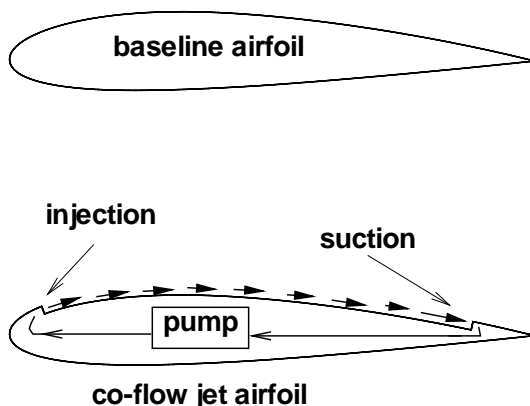


Figure 1: Baseline airfoil and CFJ Airfoil.

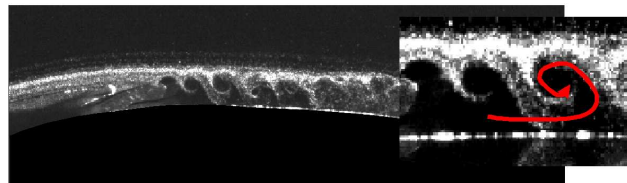


Figure 2: Coherent vortex structures in the region of CFJ airfoil injection, $AoA=5^\circ$, $C_\mu = 0.02$ [6].

The fundamental mechanism of the CFJ airfoil is that the turbulent mixing via large vortex structures between the jet and main flow energizes the wall boundary-layer. The mixing allows the flow to overcome a large adverse pressure gradient and remain attached at a very high angle of attack. Fig. 2 shows the coherent vortex structures of a CFJ airfoil observed in our wind tunnel experiment[6]. At the same time, the energized boundary layer drastically increases the circulation, augmenting lift, and reducing the total drag by filling the wake velocity deficit. The CFJ airfoil drag reduction can be so large that thrust, i.e., negative drag, is generated. The negative drag is generated at the price of the CFJ pumping power. Since the CFJ airfoil is a zero-net mass-flux(ZNMF) flow control airfoil, the drag measured in a wind tunnel is the total drag of the airfoil just as for the conventional airfoil[1]. No additional drag such as the Circulation Control airfoil will be generated.

2.1 Subsonic Low Speed Performance

Fig. 3 is the PIV measured velocity field of the CFJ-NACA-6415 airfoil at the AoA of 25° and Mach number of 0.1. It demonstrates that the flow is attached with a higher velocity within the wake than in the freestream, a reversed wake deficit. In this case, thrust is generated. Flow is attached

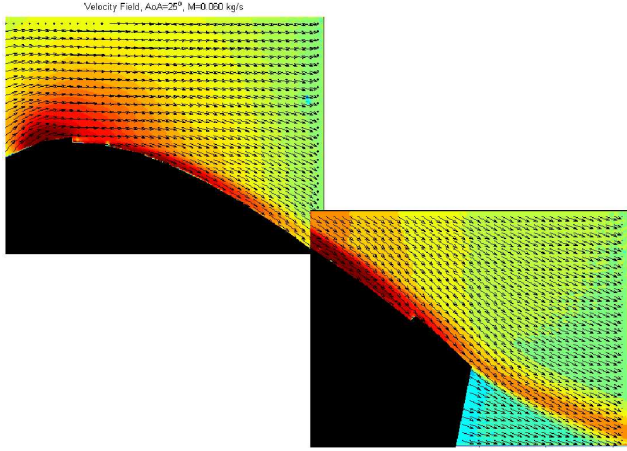


Figure 3: Attached flow of CFJ NACA 6415 airfoil at $AoA=25^\circ$ measured by PIV in experiment, $M=0.1$ [6].

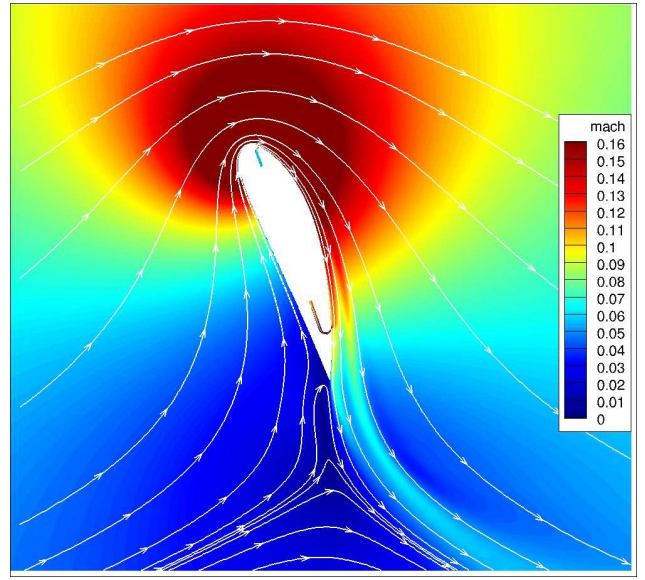


Figure 4: CFJ-NACA-6421 airfoil at $AoA=70^\circ$ with flow attached, $C_L = 10.6$, $C_\mu = 0.35$, $M=0.067$ [13].

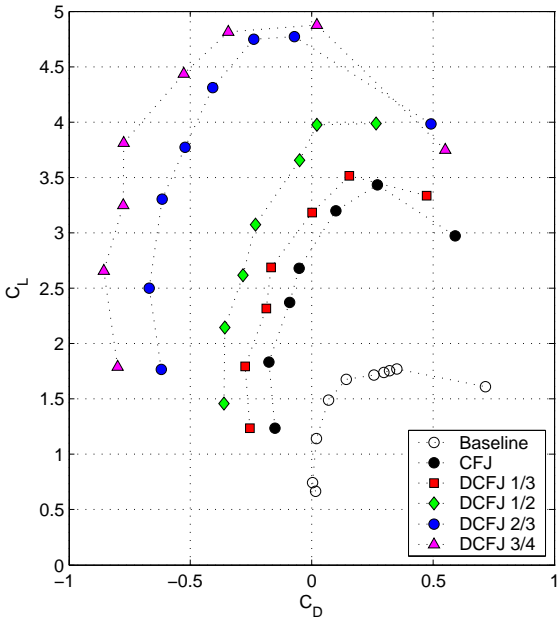


Figure 5: Measured drag polars of discrete CFJ airfoils with different obstruction factors at mass flow $\dot{m} = 0.06kg/s$ [7].

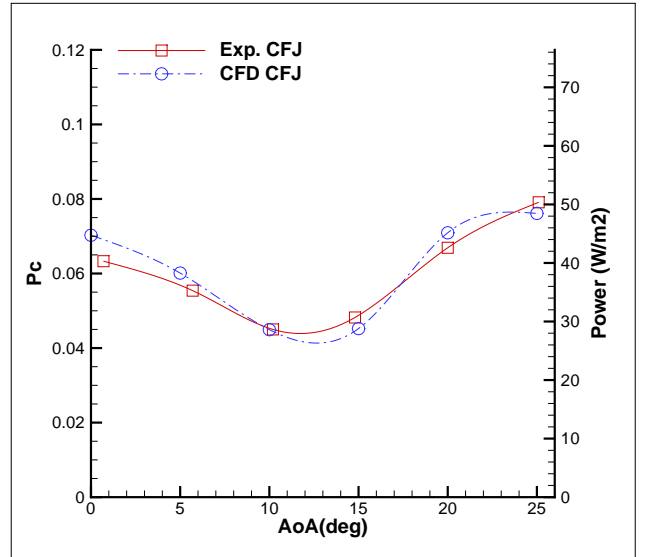


Figure 6: CFJ power coefficient comparison between CFD simulation and experiment[7].

at a momentum coefficient C_μ of 0.06 in this case. The baseline NACA-6415 airfoil has massive flow separation at AoA of 25° [6], which is completely removed by CFJ.

Fig. 4 shows that the CFJ-NACA-6421 airfoil still has attached flow at AoA of 70° with a lift coefficient C_L of 12.6, which is simulated by a well validated high order CFD code[13]. The circulation is so high that the stagnation point is detached from the airfoil body. Typically, an airfoil will get stalled at AoA of 15° with the maximum lift coefficient of 1.6. The $C_{L_{max}}$ we achieved is far greater than the

theoretical limit of maximum lift coefficient based on potential flow theory, $C_{Lmax} = 2\pi(1 + t/c) = 7.6$. We name it Super-Lift Coefficient. More details can be found in [13]. Currently, we are developing the wind tunnel tests to confirm this result under a DARPA grant[14].

Fig. 5 shows the wind tunnel test results of several CFJ airfoils at Mach number of 0.1[7]. The CFJ airfoil achieves a C_{Lmax} of about 5, more than 3 times higher than the baseline airfoil with no CFJ. It also obtains an enormous thrust coefficient of about 0.8. In other words, the CFJ airfoil can be used as a new form of distributed thrust along the wingspan while generating lift.

The CFJ airfoil has a unique low energy expenditure mechanism because the jet gets injected at the leading edge suction, where the main flow pressure is the lowest, and it gets sucked at the trailing edge, where the main flow pressure is the highest. The low energy expenditure is the key enabling the CFJ airfoil to achieve high aerodynamic efficiency and high lift coefficient at the same time for cruise condition.

Fig. 6 is the wind tunnel measured CFJ pumping power coefficient compared with the CFD prediction and they show an excellent agreement. It is observed that the power coefficient decreases with the increase of AoA up to 15° and then rises at higher AoA. When the AoA is increased and the flow still remains attached, the airfoil LE suction effect becomes stronger with lower main flow pressure near LE, and hence less power is needed to generate the injection jet with the same momentum coefficient. However, when the AoA is higher than 15° , the boundary layer momentum starts to get deteriorated and the flow separation may occur at higher AoA. The deteriorated boundary layer creates a large energy loss and the suction power is significantly increased.

In order to compare the efficiency of a CFJ airfoil with that of a conventional airfoil, a new metric, namely corrected aerodynamic efficiency $(L/D)_c$, is introduced, which takes into consideration the power needed for the CFJ[8] as the following:

$$\left(\frac{L}{D}\right)_c = \frac{L}{D + \frac{P}{V_\infty}} \quad (1)$$

where V_∞ is the free stream velocity, P is the CFJ pumping power, and L and D are the lift and drag generated by the CFJ airfoil. The $(L/D)_c$ incorporates the CFJ power consumed into the drag of the airfoil. Since the minimum CFJ pumping power occurs at a fairly high AoA as shown in Fig. 6[7, 8], the peak aerodynamic efficiency of CFJ airfoil typically has a higher AoA than conventional airfoil[8].

In [13], an aircraft productivity efficiency is introduced as C_L^2/C_D , which determines an airplane's transportation capability measured by its gross weight multiplied its maximum range under per unit fuel consumption. The CFJ airfoil can substantially increase the aircraft productivity efficiency.

2.2 Transonic Cruise Performance

The very encouraging results of the CFJ airfoil demonstrated by subsonic experiment and numerical simulation have recently been extended to transonic airfoils. Liu and Zha [12] have applied the CFJ flow control to transonic supercritical RAE2822 airfoil at cruise condition with rigorous numerical simulation that is very well validated. The Mach number is 0.729 and Reynolds number is 6.5×10^6 .

Fig. 7 is the comparison of aerodynamic efficiency $(L/D)_c$ vs C_L for the baseline supercritical airfoil and CFJ airfoil. The red solid line is for the base line airfoil, which has the peak efficiency point labeled as point 1b. The CFJ airfoil with a very low momentum coefficient C_μ of 0.001 is able to significantly increase the peak aerodynamic efficiency and lift coefficient (green dashline). The maximum improvement of the aerodynamic efficiency occurs at $C_\mu=0.003$ (purple solidline) with the peak efficiency $(L/D)_c$ significantly improved by 14.5% and the C_L improved by 18.7% simultaneously. The productivity efficiency improvement is 36%.

Both the baseline airfoil and the CFJ airfoil reach the peak efficiency at AoA of 2° . The CFJ airfoil peak efficiency starts to drop when the C_μ is greater than 0.003, but the lift coefficient continues to be increased. Comparing point 2b and point 2c, the maximum lift coefficient is improved by 26% with about the same $(L/D)_c$. Comparing point 3c and point 1b, the lift coefficient is improved by 28% with

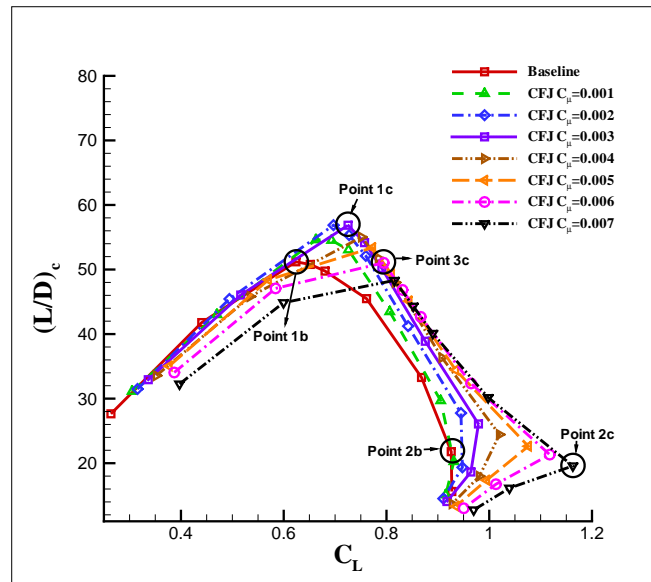


Figure 7: Aerodynamic efficiency vs C_L .

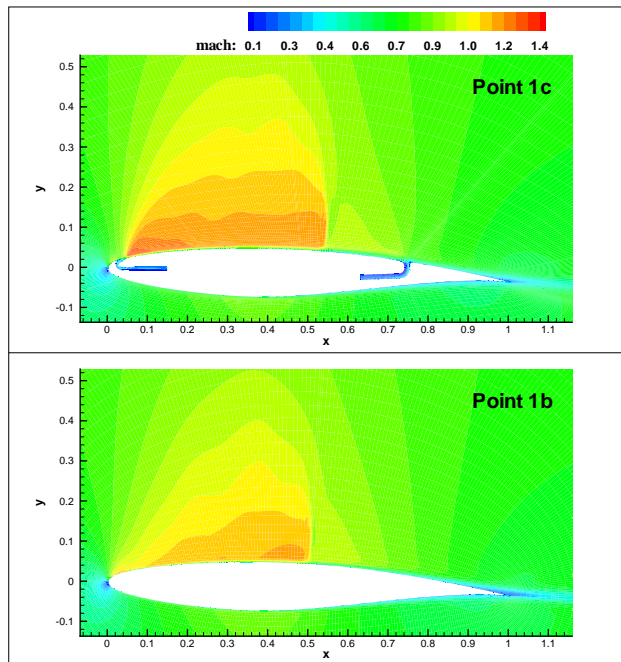


Figure 8: Mach number contours comparison for the peak efficiency condition of the transonic CFJ-RAE2822 airfoil(top) and baseline RAE2822 airfoil(bottom)[12].

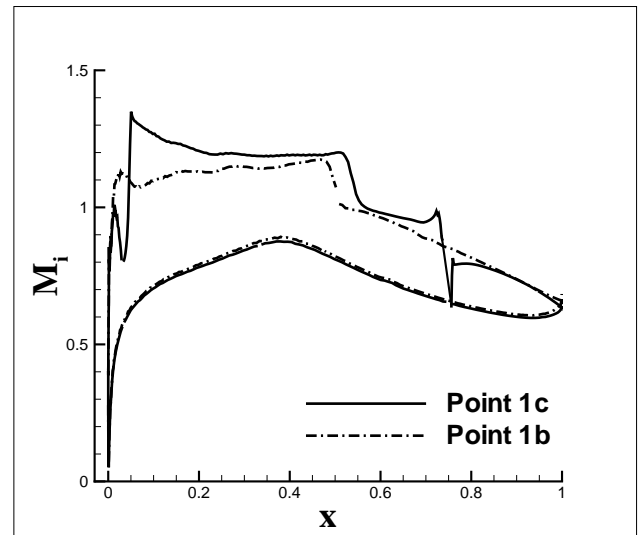


Figure 9: Surface isentropic Mach number distributions for CFJ RAE2822 airfoil ($C_{\mu}=0.003$) and baseline airfoil for the peak efficiency points.

aerodynamics efficiency (L/D)_c maintained the same. The cruise productivity efficiency is increased by 36%.

Fig. 8 compares the Mach contours for the peak efficiency points of baseline(1b) and CFJ airfoil(1c). Both are achieved at $\alpha = 2^\circ$. The Mach contours show that the CFJ airfoil expands the supersonic region to a larger area with overall higher Mach number, but still mostly less than 1.3 to achieve near isentropic compression with low wave drag.

As displayed in the surface isentropic Mach number distributions in Fig. 9, the CFJ airfoil has a

higher peak suction Mach number near the leading edge enhanced by the induction effect of the CFJ injection. The supersonic flow Mach number is then attenuated by the compression waves reflected from the sonic boundary and airfoil surface as described by Harris[15]. The normal shock of the CFJ airfoil is pushed further downstream than that of the baseline airfoil. The higher leading edge Mach number and more downstream shock location all provide the CFJ airfoil with higher lift coefficient. Even though the CFJ airfoil Mach number before the shock wave is slightly higher than that of the baseline airfoil, the shock strength is actually a little weaker with more gradual profile than that of the baseline airfoil as shown by the isentropic Mach number distribution. The Mach number right after the shock of the CFJ airfoil is closer to 1 than the baseline airfoil. This is more desirable to reduce the entropy increase as pointed out by Harris[15]. A rigorous mesh refinement study is conducted in [12] to ensure the result convergence. More detailed results of the transonic CFJ airfoil study can be seen in [12]. Currently, we are developing the wind tunnel tests to confirm this result under a DARPA grant[14].

3 Innovative Aircraft: Electric Aircraft Using Co-Flow Jet Airfoil

With the superior performance of the CFJ airfoil, the PI's team conducted a conceptual design of general aviation(GA) electric aircraft(EA) with CFJ wing[10]. The high cruise lift coefficient allows the aircraft to have a very high wing loading, allowing it to carry more batteries, hence increasing the range but keeping a compact size.

The mission requirements include four passengers, cruise at Mach 0.15, range of 314nm(361miles), at 5000ft altitude, and general dimensions similar to conventional GA. Table 1 compares some performance parameters and geometric dimensions of the CFJ electric GA with a conventional GA Cessna 172, and the state of the art electric GA, E-Genius and Taurus G4. The Taurus G4 and E-Genius were the first and second place winner of the 2011 Green Flight Challenge. The E-Genius set 7 world record as of July 2014. The wing planform area of the CFJ EA is $10.44m^2$, about 50% of that of Taurus G4 and 64% of the Cessna 172. The current level of battery energy density of 250Wh/kg is used.

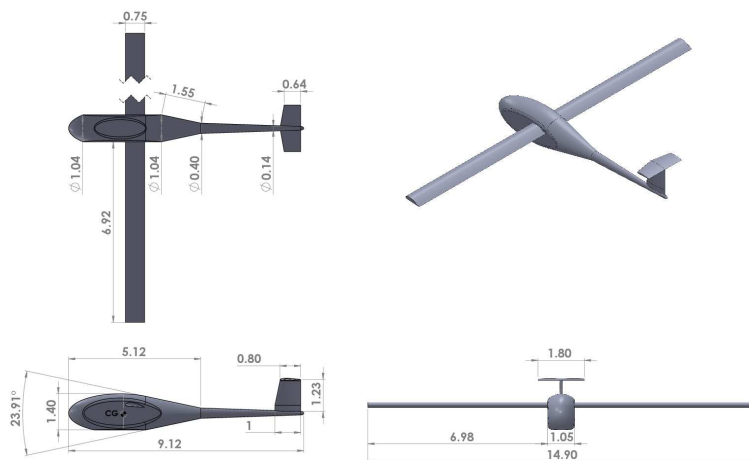


Figure 10: The CFJ EA projection views.

Fig. 10 shows three projection views and an isometric view of the CFJ EA with dimensions. The CFJ EA cruises and is trimmed at AoA of 5° . A propeller will be installed in the front. The overall propulsion efficiency is set at 73% to account for the efficiency of the propeller, controller, electric motor and gearbox. In addition, a CFJ pumping efficiency of 85% is used. A 20% of the energy storage is kept as flight reserves. Fig. 11 is the CFD calculated Mach contours at 9% span location showing the CFJ-NACA-6421 airfoil at cruise condition.

Fig. 12 shows the computed aircraft pressure contours. The CFJ-EA cruises at a very high C_L of 1.3 with CFJ momentum coefficient C_μ of 0.04. The cruise wing loading is $182.3kg/m^2$, about 3 times

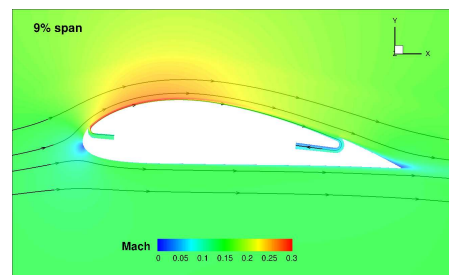


Figure 11: The CFJ EA Mach contours at 9% span location at cruise condition.

Parameter	Cessna 172	E-Genius	Taurus G4	CFJ EA
Wing span(m)	11	16.9	21.36	14.9
Planform area(m^2)	16.2	14.56	20.30	10.44
Aspect ratio	7.3	19.6	22.5	21.3
Passengers	4	2	4	4
Cruise C_L	0.32	0.57	0.5	1.31
Cruise $(L/D)_c$	7	26	28	23.5
Cruise $(C_L^2/C_D)_c$	2.24	14.82	14	30.78
Takeoff weight(kg)	1111	950	1496	1896
Battery weight(kg)	N/A	310.0	500.0	792.6
Structure factor	0.69	0.47	0.39	0.39
Wing loading(kg/m^2)	68.6	61.8	69.6	182.3
Range (nm)	700	216	250	314
MPS(Miles*Passengers/S)	172.8	29.7	49.3	120.8
Total cruise power(kw)	251.6	17.6	32	46(Prop=35.7; CFJ=10.34)
Takeoff distance(m)	519	519	610	610

Table 1: Comparison of CFJ-EA performance with other aircraft

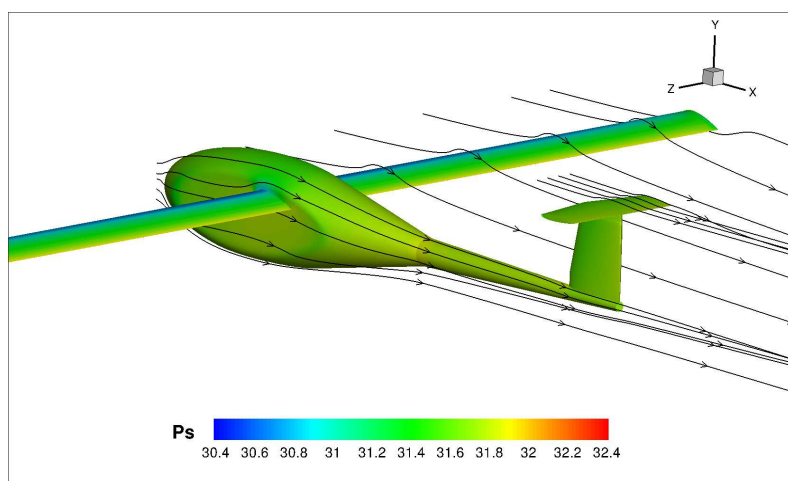


Figure 12: The CFJ EA surface pressure contours at cruise.

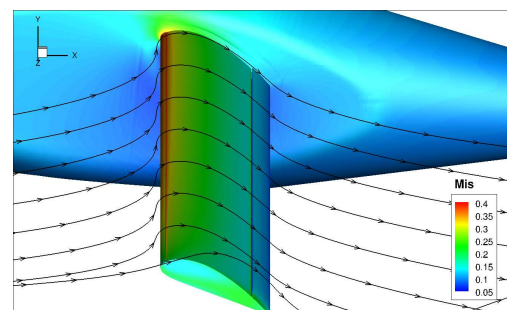


Figure 13: E-plane isentropic Mach contours at takeoff/landing at $AoA = 15^\circ$, $M=0.10$, $C_L = 3.9$, and $C_\mu = 0.24$.

higher than that of a conventional GA airplane. The aerodynamic efficiency $(L/D)_c$ is excellent with a value of 24. The net aerodynamic L/D is 36. The Takeoff and landing distances are also very good as given in Table 1 due to a very high maximum C_L of 4.8. Fig. 13 is the surface isentropic Mach contours with streamlines of the CFJ-EA at takeoff and landing conditions, which is $AoA = 25^\circ$, $C_L = 3.9$, $M=0.09$, and $C_\mu = 0.24$. The fuselage lift is enhanced by the lower stagnation region location, just under the aircraft nose, and the relatively large flow acceleration on the top surface of the cabin. The wing is significantly loaded, as indicated by the very high isentropic Mach number at the wing LE and the stagnation point located at a more downstream position on the pressure surface. The LE flow acceleration area is much smaller in the wing tip region.

Table 1 indicates that the CFJ electric GA has the productivity efficiency nearly 15 times higher than that of Cessna 172, and is more than doubled than the E-Genius and Taurus G4 that represent the state of the art electric airplane. The CFJ electric GA also has the smallest wing planform area, but has the highest total gross weight and battery weight attributed to the ultra-high cruise lift coefficient and wing loading.

A new measure of merit, $MPS = \text{Miles} * (\text{Passenger number}) / S$, where S is the wing planform area, is introduced to compare the aircraft size and their payload and range per unit area[10]. The higher the

PMS value, the more compact the aircraft, or more payload and range it can achieve for the same size. Based on Table 1, the MPS of the CFJ-EA is 2.5 to 4 times higher than those of the state of the art EA and is 70% of the Cessna 172 powered by kerosene fuel. In principle, if the aircraft is scaled up to have the same wing planform area as that of Cessna 172, the range will be 465nm(535miles). If the wing planform area is doubled to the size of Taurus G4, the range will be 568nm(654miles). Overall, the range of the CFJ-EA is at least 2 to 3 times of the same size current GA EA.

The key factor enabling this breakthrough for the enhanced range is the drastically increased cruise lift and the more than doubled productivity efficiency. This makes it possible to carry higher battery weights without having to increase the wing area with all the penalties that entails. The CFJ will be created by embedded micro-compressors inside the wing as a self-contained system. Currently, we are developing the CFJ micro-compressors under the DARPA grant[14].

4 Impacts

The cruise performance enhancement of CFJ subsonic and transonic supercritical airfoil is very encouraging. This appears to be the first significant improvement of transonic supercritical airfoil in the past five decades. It is very appealing that the CFJ airfoil is not only able to substantially increase maximum lift coefficient at low speed, but also able to improve cruise efficiency and lift coefficient for benign flows at low AoA from subsonic to transonic regime. This makes the co-flow jet airfoil unique and outstanding among the various active flow control methods. The unique superior performance of CFJ airfoil has great potential to bring the following transformative impacts and benefits to aviation industry.

1) Provide very high maximum lift coefficient without moving parts(e.g.flap system) to achieve STOL performance; 2) Significantly increase transonic cruise aerodynamic efficiency, lift coefficient and wing loading; 3) Significantly reduce the gross weight(by 30% or more); 4) Significantly increase range or reduce fuel consumption(by 30% or more) for the same payload; 5) Provide a distributed propulsion system to reduce main engine thrust, size and drag; 6) Provide a new method for yaw and lateral control with varying thrust and lift at different span location; 7) Fly high altitude with high cruise lift coefficient and high wing loading; 8) High maneuverability, high safety and fast acceleration due to the drastically increased stall AoA and CFJ thrust; and 9) Very quiet at takeoff/landing due to filled wing wake by CFJ (the owl effect).

In addition to the electric GA airplane described in section 3, we have also applied CFJ wing to develop a Mars Aerial Nuclear Global Landing Explorer(MANGLE): A Global Mobility and Multi-Mission Platform[16]. MANGLE is ranked as “One of the most important developments” in 2014 by AIAA(American Institute of Aeronautics and Astronautics). Another applications is an “Engineless” airplane propelled by CFJ wing[17]. Currently, we are conducting the research to apply the CFJ supercritical airfoil to transonic airliners. The DARPA grant [14] will make a large step forward to bring the CFJ airfoil technology to aircraft applications.

We welcome partners from industry and government to join us to advance the technology of green aviation to protect the environment of Mother Earth.

References

- [1] Zha, G.-C. and Gao, W. and Paxton, C., “Jet Effects on Co-Flow Jet Airfoil Performance,” *AIAA Journal*, No. 6,, vol. 45, pp. 1222–1231, 2007.
- [2] G.-C. Zha and D. C. Paxton, “A Novel Flow Control Method for Airfoil Performance Enhancement Using Co-Flow Jet.” *Applications of Circulation Control Technologies*, Chapter 10, p. 293-314, Vol. 214, Progress in Astronautics and Aeronautics, AIAA Book Series, Editors: Joslin, R. D. and Jones, G.S., 2006.
- [3] Zha, G.-C and Paxton, C. and Conley, A. and Wells, A. and Carroll, B., “Effect of Injection Slot Size on High Performance Co-Flow Jet Airfoil,” *AIAA Journal of Aircraft*, vol. 43, 2006.
- [4] Zha, G.-C and Carroll, B. and Paxton, C. and Conley, A. and Wells, A., “High Performance Airfoil with Co-Flow Jet Flow Control,” *AIAA Journal*, vol. 45, 2007.

- [5] Wang, B.-Y. and Haddoukessouni, B. and Levy, J. and Zha, G.-C., “Numerical Investigations of Injection Slot Size Effect on the Performance of Co-Flow Jet Airfoil ,” *AIAA Journal of Aircraft*, vol. 45, pp. 2084–2091, 2008.
- [6] B. P. E. Dano, D. Kirk, and G.-C. Zha, “Experimental Investigation of Jet Mixing Mechanism of Co- Flow Jet Airfoil.” AIAA-2010-4421, (5th AIAA Flow Control Conference, Chicago, IL), 28 Jun - 1 Jul 2010.
- [7] B. P. E. Dano, G.-C. Zha, and M. Castillo, “Experimental Study of Co-Flow Jet Airfoil Performance Enhancement Using Micro Discreet Jets.” AIAA Paper 2011-0941, 49th AIAA Aerospace Sciences Meeting, Orlando, FL,, 4-7 January 2011.
- [8] Lefebvre, A. and Dano, B. and Bartow, W. and Di Franzo, M. and Zha, G.-C., “Performance and Energy Expenditure of Co-Flow Jet Airfoil with Variation of Mach Number,” *AIAA Journal of Aircraft*, vol. 53, pp. 1757–1767, 2016.
- [9] Lefebvre, A. and Zha, G.-C., “Numerical Simulation of Pitching Airfoil Performance Enhancement Using Co-Flow Jet Flow Control.” AIAA Paper 2013-2517, AIAA Applied Aerodynamics Conference, San Diego, CA, 24 - 27 June 2013.
- [10] Lefebvre, A. and Zha, G.-C. , “Design of High Wing Loading Compact Electric Airplane Utilizing Co-Flow Jet Flow Control.” AIAA Paper 2015-0772, AIAA SciTech2015: 53nd Aerospace Sciences Meeting, Kissimmee, FL, 5-9 Jan 2015.
- [11] Lefebvre, A. and Zha, G.-C., “Trade Study of 3D Co-Flow Jet Wing for Cruise and Takeoff/Landing Performance.” AIAA Paper 2016-0570, AIAA SCITECH2016, AIAA Aerospace Science Meeting, San Diego, CA, 4-8 January 2016.
- [12] Liu, Z.-X. and Zha, G.-C., “Transonic Airfoil Performance Enhancement Using Co-Flow Jet Active Flow Control.” Proceedings of the AIAA Aviation 2016, the 8th AIAA Flow Control Conference, June 13-17, 2016.
- [13] Yang, Y.-C. and Zha, G.-C., “Super-Lift Coefficient of Active Flow Control Airfoil: What Is the Limit?.” AIAA Paper 2017-1693, AIAA SCITECH2017, 55th AIAA Aerospace Science Meeting, Grapevine, Texas, 9-13 January 2017.
- [14] Zha, G.-C., Cattafesta, L. and Kumar, R. and Bowersox, R. and White, E., “ESTOL Performance for Heavy Lift Transports Using Ultra-High Lift High Efficiency Co-Flow Jet Airfoil.” DARPA Contract HR0011-16-2-0052, 09/20/2016 - 09/19/2017.
- [15] C. D. Harris, “NASA Supercritical Airfoils.” NASA Technical Paper 2969, 1990.
- [16] Zha, G.-C. and Haefner, K. M. and Hayton, B. M. and Ding, M., “Mars Aerial Nuclear Global Landing Explorer: A Global Mobility and Multi-Mission Platform.” AIAA Paper 2014-3820, 50th AIAA/ASME/SAE/ASEE Joint Propulsion Conference, Cleveland, OH, 28 - 30 July 2014.
- [17] J. Aguirre and G.-C. Zha, “Design and Study of “Engineless” Airplane Using Co-Flow Jet Airfoil.” AIAA Paper 2007-4441, June 2007.